IOP Conf. Series: Materials Science and Engineering **202** (2017) 012090 doi:10.1088/1757-899X/202/1/012090

The Structure, Magnetic and Absorption Properties of Zn-Ti Substituted Barium-Strontium Hexaferrite Prepared by Mechanochemical Process

D S Winataputra[1], T L Ujiyanti[2] and W A Adi[1]

[1]Centre for Science and Technology of Advanced Materials, National Nuclear Energy Agency
Kawasan Puspiptek Serpong, Tangerang Selatan – Indonesia 15313
[2]Study Program of Physics, Faculty of Science and Technique, Purwokerto University, Central Java – Indonesia

Email:didinsw@batan.go.id

Abstract. Synthesis and characterization of $(Ba,Sr)_{0.5}Fe_{12-x}Zn_xTi_xO_{19}$ M-type hexaferrite was conducted by using mechanochemical process. The composition of Zn-Ti ion in $(Ba,Sr)_{0.5}Fe_{12-x}Zn_xTi_xO_{19}$ M-type hexaferrite were varied as x = 0.0, 0.2, 0.6, and 1.0. The sample was characterized by using X-rays diffractometer (XRD), scanning electron microscope (SEM), vibrating sample magnetometer (VSM), and vector network analyzer (VNA). The XRD patterns were further analyzed by Rietveld analysis program. The Rietveld analysis result indicated that the substitution of Zn-Ti ions led to the expansion of the hexagonal lattice parameter and unit cell volume (V_{cell}), while the atomic density decreased with increasing of the Zn-Ti ion. The VSM measurement exhibited that the substitution of the Zn-Ti ions caused the change in magnetic properties behavior such as intrinsic magnetic coercivity (H_{ci}), remanence (M_r) and saturation (M_s) magnetization. The value of H_c dropped significantly with the substitution of Zn-Ti ions, and then continued to decrease with the addition of Zn-Ti ions content for x = 0.6, and x = 1.0. SEM observation revealed that all the particles showed nearly hexagonal platelet shape, with the particle size distribution at most in the range between 200 – 600 nm. The variation of the reflection loss versus frequency was measured by using VNA in $(Ba,Sr)_{0.5}Fe_{12-x}(ZnTi)_xO_{19}$ hexaferrite for x= 0.0 – 1.0. The optimum reflection loss (RL) was found to be –48 dB at 14 GHz in $(Ba,Sr)_{0.5}Fe_{11.6}(ZnTi)_{0.2}O_{19}$ hexaferrite for x = 0.2.

Keywords: $(Ba,Sr)_{0.5}Fe_{12-x}Zn_xTi_xO_{19}$, M-type hexaferrite, Zn-Ti ions substitution, magnetic property, reflection loss.

1. Introduction

Barium hexaferrite is one of M-type hexaferrites. Barium hexaferrite has a large saturation magnetization, high coercivity, high Curie temperature, large uniaxial magnetic crystalline anisotropy, and excellent chemical stability. Therefore, Barium hexaferrite is promising candidates for the development of microwave absorbing materials [1–3]. Barium hexaferrite has significantly large crystalline anisotropy due to their low crystal symmetry, as it is compared with the cubic symmetry of spinel or garnet ferrites. Therefore, the resonance frequency can reach as high as GHz [4–6].

Furthermore, the location of resonance can be modified over a wide frequency range by the substitution of ions in Barium hexaferrite.

Many reports are available for the synthesis and characterization of the barium hexaferrite substituted with various cations like Sr, Pb, La for Ba and Mn-Ti, Co-Ti, Ni-Cr for Fe [7–11]. These studies revealed that the structural, magnetic, and microwave absorbing properties of barium hexaferrite are strongly influenced by the substitution of multivalent cations. Therefore, this research focused on the effect of the ions substitution on the structure, magnetic and absorbing behavior in $(Ba,Sr)_{0.5}Fe_{(12-2x)}(ZnTi)_xO_{19}$ (for x = 0.0, 0.2, 0.6, 1.0) hexaferrite. The main objectives are to fabricate $(Ba,Sr)_{0.5}Fe_{(12-2x)}(ZnTi)_xO_{19}$ (for x = 0.0, 0.2, 0.6, 1.0) using the mechanochemical method and investigate the influence of Zn-Ti ions doping concentration in composites on the structural, magnetic and microwave absorbing performance.

The synthesis was done through a mechanochemical process. The obtained materials then characterized by using X-ray diffractometer (XRD), scanning electron microscope (SEM), and vibrating sample magnetometer (VSM) to study the samples' microstructure, and magnetic properties. The characterization of reflection and transmission of microwave were carried out by using the Vector Network Analyzer (VNA, ADVANTEST R3770) with a frequency ranged from 7 to 15 GHz.

2. Experimental Method

As starting materials of titanium dioxide (TiO_2), zinc oxide (ZnO_2), hematite (α-Fe_2O_3), barium carbonate ($BaCO_3$), and strontium carbonate ($SrCO_3$) were used. A series of $(Ba,Sr)_{0.5}Fe_{12-x}Zn_xTi_xO_{19}$ samples with x = 0.0, 0.2, 0.6, and 1.0 were synthesized with a mechanochemical method using HEM, Certi-prep 8000 mixer [12,13]. The prepared for doped samples were mixed together in a stainless steel vial. The ground mixing of each sample was performed for 5 hours. The ball and sample weight ratio was 10 : 1. Furthermore, the sample was dried in an oven at 80 ºC, and followed by sintering at 1000 °C for 5 hours.

The crystalline structure was determined by using X-ray diffractometer (XRD, Philips Pan-analytical Empyrean) using Cu-Kα radiation (λ = 15.405 nm) in the range of 20 –70^o of 2θ. The XRD data was analyzed by using general structure analysis system (GSAS) program [14]. The morphology of the sample was characterized by using a scanning electron microscope (SEM, JEOL-JSM 6510). The magnetic measurements were carried out with a vibrating sample magnetometer (VSM, Oxford 1.2T) at a room temperature. The reflection loss of the absorber was measured by using microwave Network Analyzer (ADVANTEST R3770) in the frequency range of 7 – 15 GHz.

3. Result and Discussion

3.1 Structure Properties

Figure 1 shows the XRD patterns of Fe_2O_3 and $(Ba,Sr)_{0.5}Fe_{12-x}Zn_xTi_xO_{19}$ (x = 0.0, 0.2, 0.6, and 1.0). Based on Figure 1(a) and 1(b), $(Ba,Sr)_{0.5}Fe_{12-x}Zn_xTi_xO_{19}$ without and with Zn and Ti doping for x = 0.2 were identified to be single phase. The diffraction peaks of M-type $BaFe_{12}O_{19}$ hexaferrite phase in Figure 1 are marked by "+". However, with the addition of Zn-Ti ions doping for x = 0.6 and 1.0, the figure shows the broadened diffraction peaks corresponding to Fe_2O_3 hematite phase (signed by " • "), see Figure 1(c) and 1(d).

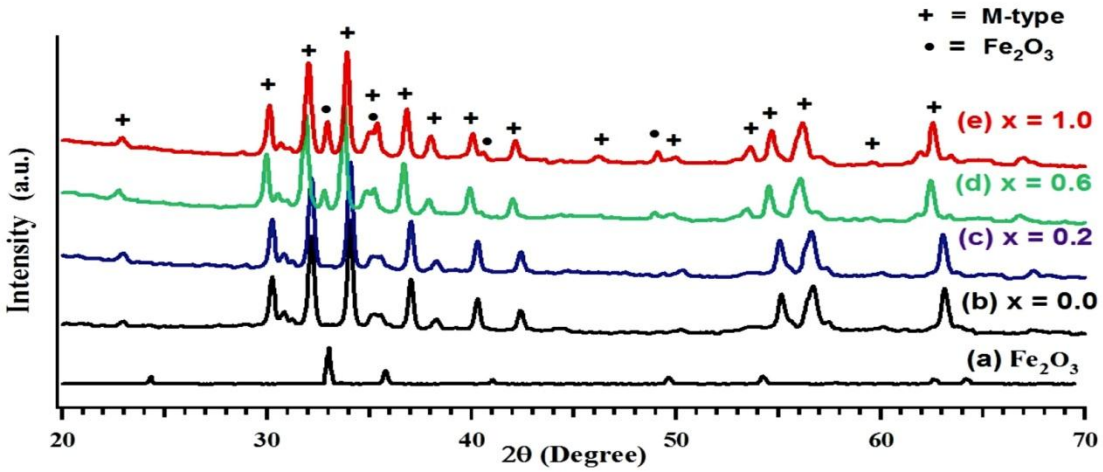

Figure 1. XRD pattern of Fe_2O_3 (a), $(Ba,Sr)_{0.5}Fe_{12-x}Zn_xTi_xO_{19}$ powder for (b) x = 0.0, (c) x = 0.2, (d) x = 0.6, and (e) x = 1.0 after heat treated at 1000 ^oC for 5 h.

Figure 2 shows SEM pictures of $(Ba,Sr)_{0.5}Fe_{12-x}Zn_xTi_xO_{19}$ powder (x = 0.0, 0.2, 0.6, and 1.0) prepared by mechanochemical method after sintering at 1000 °C for 5 h in the air atmosphere. From Figures 2 for all SEM images, it can be seen that the particle inside the sample was grown with relatively uniform shape. In Figure 2(a), the particles were nearly spherical-like shape. The particle size distribution was almost evenly and smaller than 600 nm. In Figure 2(b), 2(c), and 2(d), it is seen that the particle showed nearly platelet shape. However, it is clear that the particle size was smaller below 1000 nm.

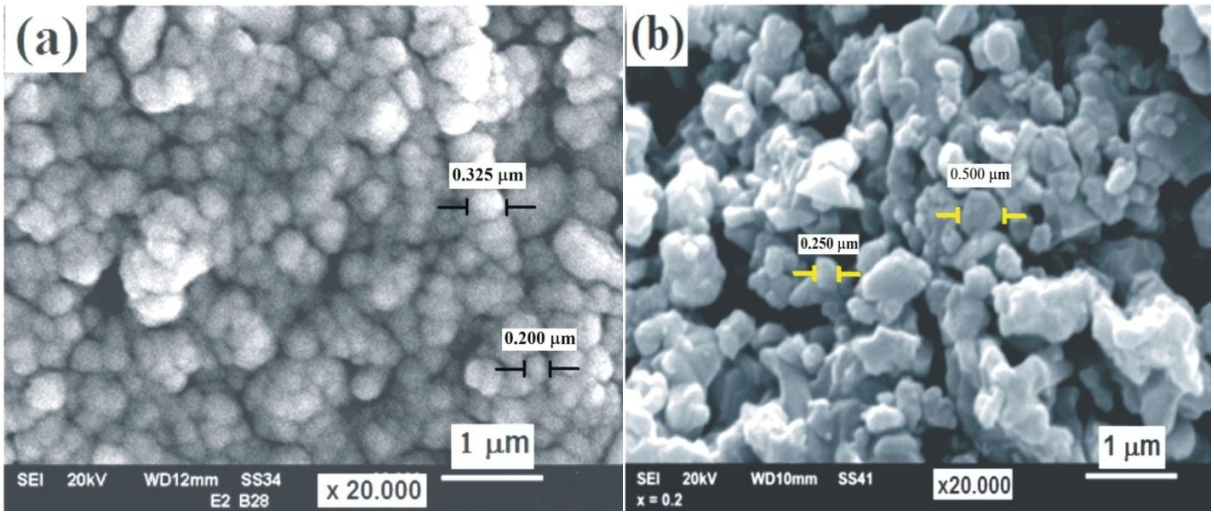

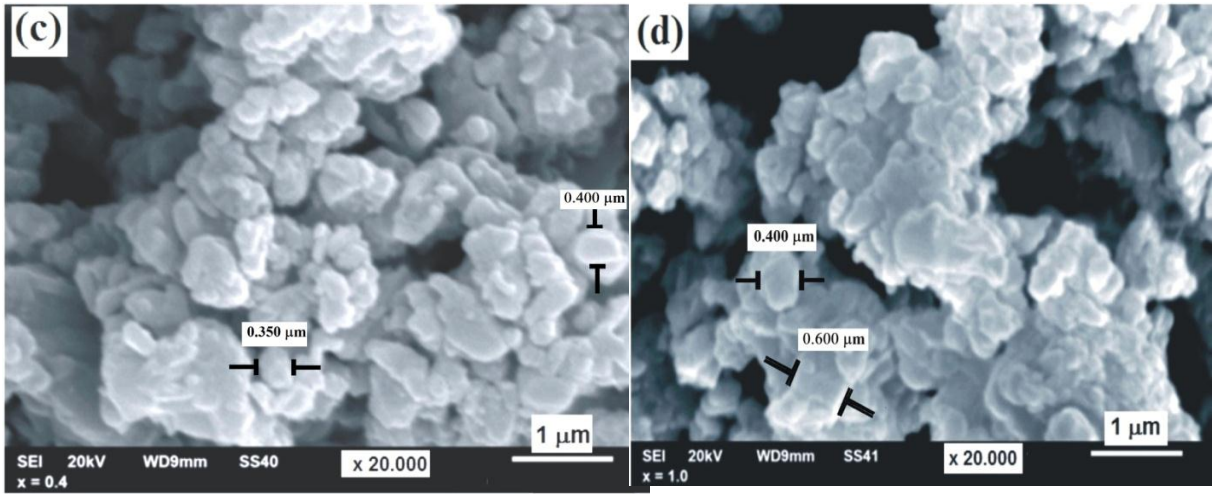

Figure 2. The morphology of $(Ba,Sr)_{0.5}Fe_{12-x}Zn_xTi_xO_{19}$ powder for (a) x = 0.0, (b) 0.2, (c) 0.6, and (d) 1.0.

Figure 3 shows the refinement result of XRD pattern of $(Ba,Sr)_{0.5}Fe_{12-x}Zn_xTi_xO_{19}$ samples without and with Zn-Ti doping for x = 0.0, 0.2, 0.6, and 1.0. The refinement result produced a very good quality of fitting with *R* factor and goodness of fit value χ^2 (chi-squared) was less than 1.2, as shown in Table 1. From Figure 3, the plus symbol (+) of red line represents the observation, while the green line is the calculation. Miller index is signed by bar symbol (I) and the difference between observation and calculation is represented by purple line symbol (-). Based on Figure 3(a), and 3(b), it can be seen that $(Ba,Sr)_{0.5}Fe_{12-x}Zn_xTi_xO_{19}$ (for x = 0.0, and x = 0.2) were identified to be single phase hexagonal structure, indicating the doping elements had been substituted into the structure successfully. The diffraction pattern produced in accordance with JCPDS # 84-1531 and the space group was $P6_3/mmc$.

A little change has been found in Figure 2(b) and 2(c) which show the peak broadening and corresponding to the impurities phase, which may be due to the difference in the molarities of the precursor. The content of impurities phase was obtained from the analysis by using GSAS program is listed in Table 1. Based on the Table 1, about 70% and 60% phase purities were achieved with substitution of Zn-Ti ions for x = 0.6 and x = 1.0 respectively. Earlier studies reported that the impurities such as Fe_2O_3 phase begin to dissolve at the temperature greater than 1000 ^oC. It helps aggregation of the particles and grains growth significantly during sintering process [1,12].

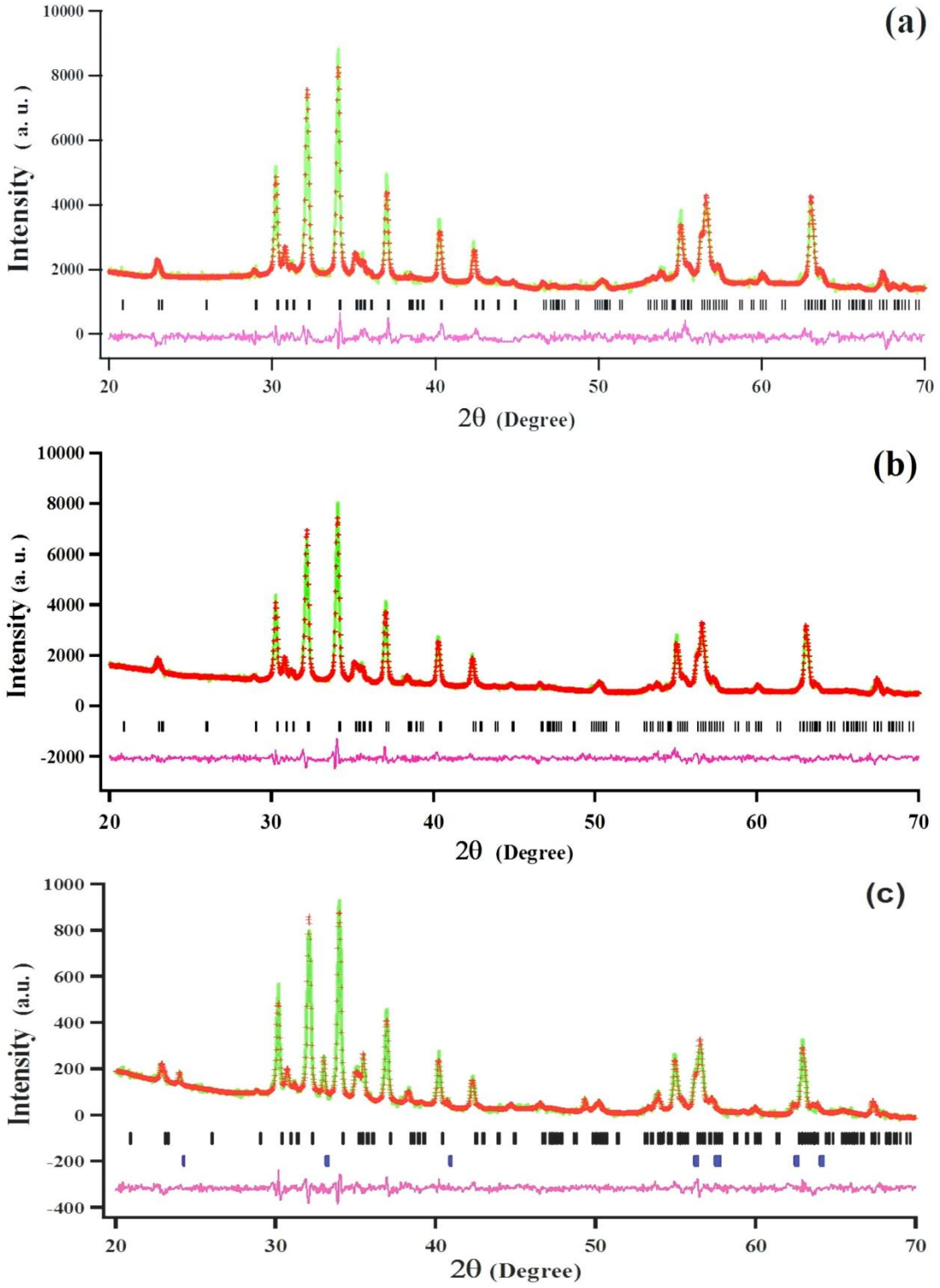
(a)
Intensity (a. u.)
2θ (Degree)
(b)
Intensity (a. u.)
2θ (Degree)
(c)
Intensity (a.u.)
2θ (Degree)

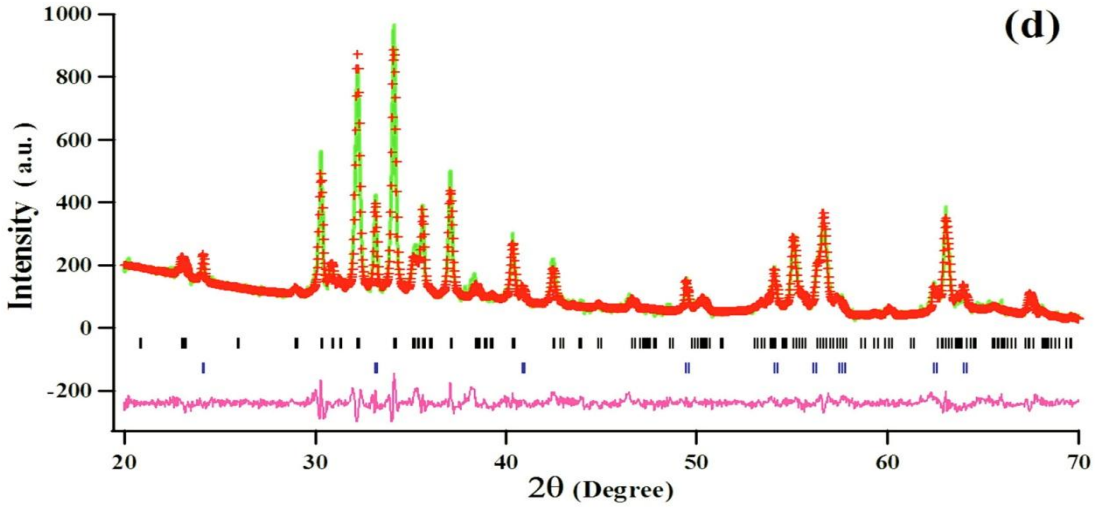

Figure 3. The refinement XRD pattern of $(Ba,Sr)_{0.5}Fe_{12-x}Zn_xTi_xO_{19}$ powder for (a) x = 0.0, (b) x = 0.2, (c) x = 0.6, and (d) x = 1.0.

Table 1. Phase quantification after Rietveld analysis on the XRD patterns of $(Ba,Sr)_{0.5}Fe_{12-x}Zn_xTi_xO_{19}$

Comp. "*x*"	$(Ba,Sr)_{0.5}Fe_{(12-2x)}(ZnTi)_xO_{19}$ Hexaferrite	Phase (%)	
		$(Ba,Sr)_{0.5}Fe_{12}O_{19}$	Fe_2O_3
0.0	$(Ba,Sr)_{0.5}Fe_{12}O_{19}$	100.00	0.00
0.2	$(Ba,Sr)_{0.5}Fe_{11.6}(ZnTi)_{0.2}O_{19}$	100.00	0.00
0.6	$(Ba,Sr)_{0.5}Fe_{10.8}(ZnTi)_{0.6}O_{19}$	77.00	23.00
1.0	$(Ba,Sr)_{0.5}Fe_{10.0}(ZnTi)_{1.0}O_{19}$	67.00	33.00

Variation of lattice parameters (*a, c*), volume cell and atomic density as a function of Zn-Ti content is shown in Figure 4. It appears that the value of *a* and *c* are slightly increased with increasing the Zn-Ti contents as indicated by Figure 4a. The effect of Zn-Ti ions doping also led to increase the unit cell volume (V_{cell}) is quite significant, especially for x = 1.0, while the atomic density decreases as depicted in Figure 4(b). It indicated that the regular structure became slightly elongated along *a*-axis and *c*-axis. As a result, the dopant ions changed both of the lattice parameters, cell volume, and atomic density.

The atomic substitution of Fe^{2+}/Fe^{3+} by Zn^{2+}/Ti^{4+} has a significant impact on the lattice parameters. Energy perturbation and lattice distortion were expected when Fe^{2+}/Fe^{3+} were replaced by Zn^{2+}/Ti^{4+} ions due to the difference in their atomic radii and their orbitals. This condition caused the anisotropy energy to change, and thus the magnetic behavior changed particularly coercivity which decreased with Zn/Ti doping, as shown in Figure 5. The observed variation depended on the difference in the ionic radii of the metal ions Zn = 0.74 Å, Ti = 0.68 Å compare to Fe = 0.645 Å.

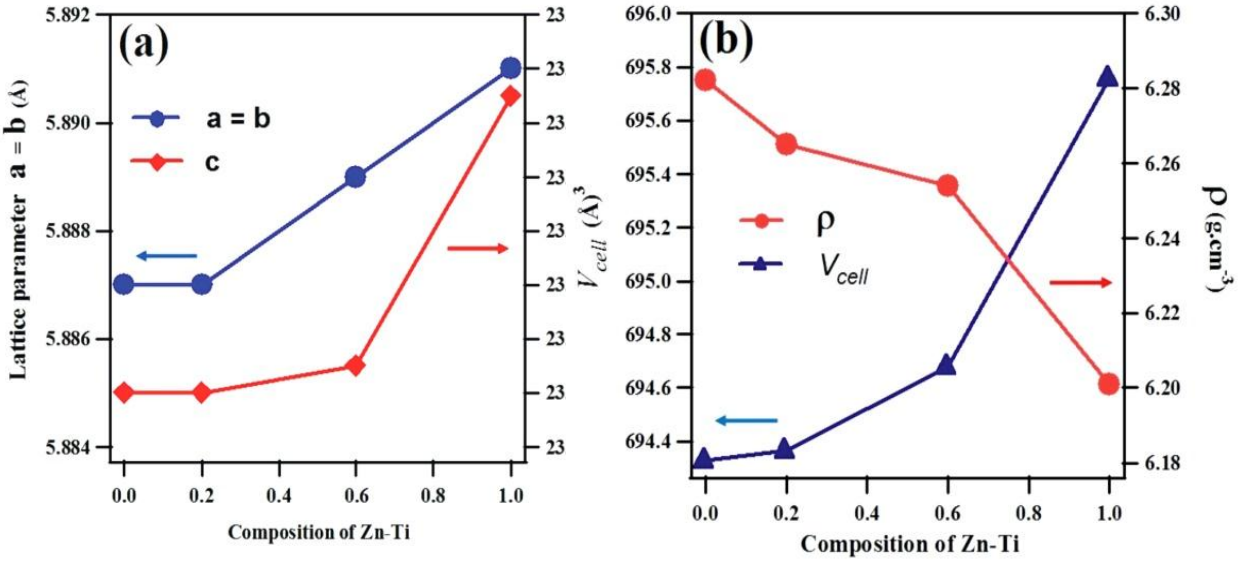

Figure 4. The plot of (a) lattice parameter (*a,c*), and (b) V_{cell} and atomic density as a function of composition of Zn-Ti.

3.2 Magnetic Properties

Figure 5 represents the sequences hysteresis loop behavior of $(Ba,Sr)_{0.5}Fe_{12-x}(ZnTi)_xO_{19}$ powder with variation of Zn-Ti ions doping for x = 0.0, 0.2, 0.6, and 1.0. The characteristic magnetic parameters are listed in Table 2. The variations of M_s, M_r, and H_c values of $(Ba,Sr)_{0.5}Fe_{12-x}(ZnTi)_xO_{19}$ are shown in Figure 5(b), 5(c), and 5(d). It is seen that the substitution of the Zn-Ti ions caused decrease significantly in intrinsic coercivity, H_{ci} and little affected to saturation magnetization, Ms at low substitution. Based on Table 2, H_c was observed to be 4.0 kOe in the unsubstituted sample. A small amount of Zn-Ti ions doping (for x = 0.2) did not significantly affect the structure but had a great influence on magnetic properties. The M_s value remained almost constant, but H_c rapidly decreased from 4.00 kOe to 2.35 kOe. As x continued to increase to x = 1.0, the value of M_s and Hc decreased to 74 emu/g, and H_c to 1.00 kOe, respectively. Magnetic remanent, M_r also decreased with the increase of ions substitution. The decrease in M_r was due to the net alignment of grain magnetization caused by weak inter-grain exchange interactions. The high value of H_c in undoped sample was due to uniaxial magnetocrystalline anisotropy along *c*-axis. C-axis is very sensitive to magnetic properties and anisotropy of Ba-hexaferrite and is responsible for coercivity. Thus, the increase in *c*-axis with the addition of "x" alters the distance between magnet ions, so that the exchange interaction varies which in turn changes the magnetic properties.

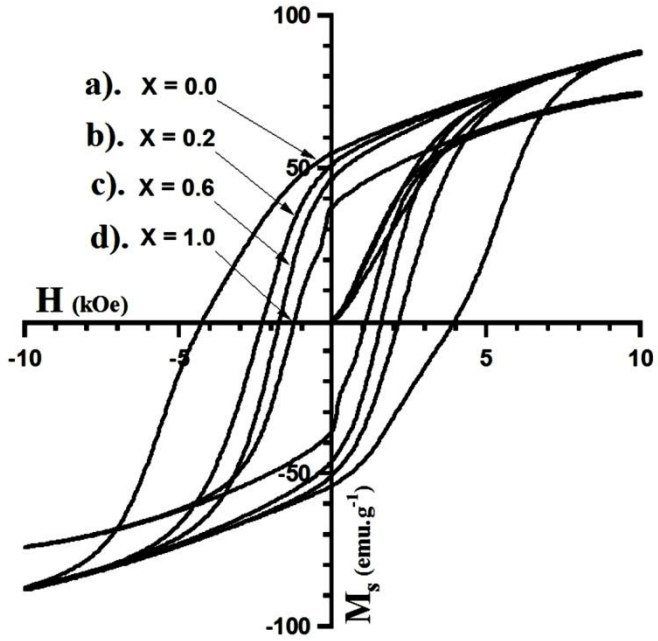

Figure 5. Room temperature hysteresis loop of $(Ba,Sr)_{0.5}Fe_{(12-2x)}$ $(ZnTi)_xO_{19}$ powder sample for (a) x = 0.0, (b) x = 0.2, (c) x= 0.6, and (d) x=1.0.

Table 2 Magnetic properties of $(Ba,Sr)_{0.5}Fe_{12-x}Zn_xTi_xO_{19}$ as a function of Zn-Ti substitution level x.

Comp. "x"	$(Ba,Sr)_{0.5}Fe_{(12-2x)}(ZnTi)_xO_{19}$ Hexaferrite	H_{ci} (kOe)	emu.g^{-1}	
			M_s	M_r
0.0	**$(Ba,Sr)_{0.5}Fe_{12}O_{19}$**	4.00	88.20	53.50
0.2	**$(Ba,Sr)_{0.5}Fe_{11.6}(ZnTi)_{0.2}O_{19}$**	2.35	88.20	50.10
0.6	**$(Ba,Sr)_{0.5}Fe_{10.8}(ZnTi)_{0.6}O_{19}$**	1.60	87.60	45.30
1.0	**$(Ba,Sr)_{0.5}Fe_{10.0}(ZnTi)_{1.0}O_{19}$**	1.10	74.70	34.90

3.3 Absorption Characteristics

Figure 6 (a-d) shows the variation of the reflection loss versus frequency, observed in $(Ba,Sr)_{0.5}Fe_{12-x}(ZnTi)_xO_{19}$ hexaferrite (for x = 0.0, 0.2, 0.6 and 1.0) at a thickness of 2 mm and in the frequency range of 7–15 GHz. The minimum value of the reflection loss exhibited a peak at approximately −10 dB at a frequency of 7 GHz for x = 0.0 (undoped) sample. For x = 0.2 (Figure 6b), the reflection loss exhibited two peaks at approximately −44 dB at a frequency of 8 GHz and -48 dB at 14 GHz, with a bandwidth of 0.5 GHz. For x = 0.6 (Figure 6c), the reflection loss also exhibited two peaks at approximately −22 dB and -26 dB at 8 GHz and 14.5 GHz. With the addition of Zn-Ti substitutions for x = 1.0 (Fig. 6d), the reflection loss exhibited three peaks approximately at -32 dB at 8 GHz, -34 dB at 11 GHz and -44 dB at 14 GHz.

The optimum reflection loss was found to be –48 dB at a frequency of 14 GHz in $(Ba,Sr)_{0.5}Fe_{11.6}(ZnTi)_{0.2}O_{19}$ hexaferrite for x = 0.2 (Figure 6b). The Zn-Ti substitution to Fe site affected to domain wall pinning and the change of magnetic anisotropy, so that the damping of domain turning and domain wall displacement increases, thus leading to the resonance enhancement and resonance frequency-position shift [6,9,15]. However, an excessive amount of ions doping may result in weak microwave absorption, due to the increase in electric resistivity. As a result, a suitable amount of Zn-Ti doping is required to improve the microwave absorption of M-type barium hexaferrite.

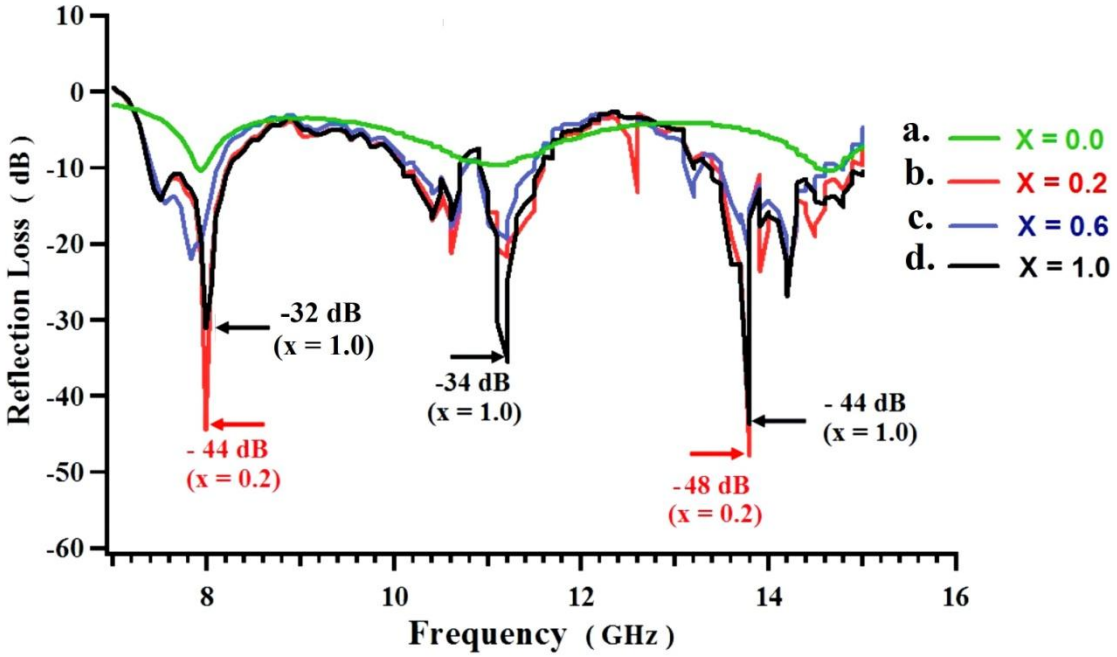

Figure 6. The absorption characteristics of the $(Ba,Sr)_{0.5}Fe_{12-x}(ZnTi)_xO_{19}$ hexaferrite for x at (a) 0.0, (b) 0.2, (c) 0.6, and (d) x =1.0.

4. Conclusion

M-type hexaferrite of $(Ba,Sr)_{0.5}Fe_{12-x}Zn_xTi_xO_{19}$ (for x = 0.0, 0.2, 0.4, 0.6, 1.0) has been synthesized through mechanochemical process. The structural, magnetic and absorption properties of the synthesized composition were studied by using XRD, SEM, VSM and VNA. The refinement of XRD pattern results showed that the M-type hexaferrite for x = 0.0 and x = 0.2 are single phase. The phase purity decreased with the increase of Zn-Ti concentration for x = 0.6 and x = 1.0. The effect of the Zn-Ti ions substitution led changes in the structural and magnetic properties. The lattice parameter increased became elongated along *a* and *c*-axis with the doping of Zn-Ti, and also led to increase the unit cell volume (V_{cell}). The magnetic properties behaviors such as magnetic coercivity, remanent and saturation magnetization led to decrease, as the addition of Zn-Ti substitution. The Effect doping of Zn-Ti could enhance the impedance matching and microwave attenuation, which the optimum reflection loss was found to be –48 dB at 14 GHz in $(Ba,Sr)_{0.5}Fe_{11.6}(ZnTi)_{0.2}O_{19}$ for x = 0.2.

5. References

[1] L Jie, Huai-Wu Z, Yuan-Xun L, Ying-Li L and M. Yan-Bing. 2012 The Structural and Magnetic Properties of Barium Ferrite Powders Prepared by Sol-gel Method *Chin Phys B* **21** 17501-017501–4

[2] Jesús F S 2014 Mechanosynthesis , crystal structure and magnetic characterization of M-type *Ceram. Int.* **40** 4033–8

[3] Trukhanov A V, Panina L V, Trukhanov S V, Turchenko V O, Kazakevich I S and Salem M M 2015 Features of Crystal Structure and Magnetic Properties of M-type Ba-hexaferrites with Diamagnetic Substitution *Int. J. Mater. Chem. Phys.* **1** 286–94

[4] Kaur R and Aul G D 2012 Effect of Reflection Property on Microwave Absorbing Materials - A Review *Int. J. Sci. Res. IJSR*

[5] Li C-J, Wang B and Wang J-N 2012 Magnetic and Microwave Absorbing Properties of Electrospun Ba(1−x)LaxFe12O19 Nanofibers *J. Magn. Magn. Mater.* **324** 1305–11

[6] Qin X, Cheng Y, Zhou K, Huang S and Hui X 2013 Microwave Absorbing Properties of W-Type Hexaferrite Ba(MnZn)xCo2(1−x)Fe16O27 *J. Mater. Sci. Chem. Eng.* **1** 8–13

[7] Haq A and Anis-ur-Rehman M 2012 Effect of Pb on Structural and Magnetic Properties of Ba-Hexaferrite *Pysica B* **407** 822–6
[8] Li W, Qiao X, Liu M and Peng H 2013 La and Co Substitutwd M-tpe Barium Ferrites Processed by Sol-gel Combustion Synthesis *Mater. Res. Bull.* **48** 4449–53
[9] Kanagesan, S, Mansor H and Sinnappan J 2014 Microwave Sintering of Zn-Nb Doped Barium Hexaferrite Synthesized via Sol-Gel Method *Mater. Sci. Appl.* **5** 171–6
[10] Ali-Sharbati, Saeed-Choopani, Ali-Ghasemi, Al-amri A, Cerqueira C F and JR. A P 2011 Synthesize and Magnetic Propertiesof of Nanocrystalline Ba3 Co2 (0.8- x) Mn0.4 Ni2x Fe24 O41 Prepared by Citrate Sol-gel Method *Digesr J. Nanomater. Biostructures* **6** 187–98
[11] González-Angeles A, Lipka J, Grusková A, Sláma J, Jančárik V and Slugeň V 2010 Magnetic comparison of BaCa and BaSr substituted hexaferrite powders *J. Phys. Conf. Ser.* **217** 12137
[12] Adi W A and Manaf A 2012 Structural and Absorption Characteristics of Mn-Ti Substituted Ba-Sr Hexaferrite Synthesized by Mechanical Alloying Route *J Basic Appl Sci Res* **2** 7826–34
[13] Ujiyanti T. L. 2014 Synthesis and Characterization of (Ba,Sr)0.5Fe12-x(ZnTi)xO19, (x = 0.2, 0.4, 0.6, and 1.0 wt %) as Electromagnetic Wave Absorber *Bachelor Thesis* 2014
[14] Larson A C and Von Dreele R B 2004 *GENERAL STRUCTURE ANALYSIS SYSTEM (GSAS), Los Alamos National Laboratory Report LAUR (2004), pp. 86-748* .
[15] Vinayasree S, Soloman M A, Sunny V, Mohanan P, Kurian P, Joy P A and Anantharaman M R 2014 Flexible microwave absorbers based on barium hexaferrite, carbon black, and nitrile rubber for 2-12GHz applications *J. Appl. Phys.* **116**

Acknowledgements
This research was supported by "Research and Development of Smart magnetic and Magnetic Oxide Programme for DIPA Grants 2016" at Centre for Science and Technology of Advanced Materials – National Nuclear Energy Agency, Republic of Indonesia.